Behavior of the N-Terminal Helices of the Diphtheria Toxin T Domain during the Successive Steps of Membrane Interaction †

ARTICLE *in* BIOCHEMISTRY · MARCH 2007

Impact Factor: 3.02 · DOI: 10.1021/bi602381z · Source: PubMed

8 AUTHORS, INCLUDING:

Caroline Montagner
University of Liège
9 PUBLICATIONS **134** CITATIONS
SEE PROFILE

Daniel Gillet
CEA - Atomic and Alternative Energies Comm…
75 PUBLICATIONS **1,341** CITATIONS
SEE PROFILE

Alexandre Chenal
Institut Pasteur
57 PUBLICATIONS **1,074** CITATIONS
SEE PROFILE

Behavior of the N-Terminal Helices of the Diphtheria Toxin T Domain during the Successive Steps of Membrane Interaction†

Caroline Montagner,‡,§ Aurélie Perier,||,§ Sylvain Pichard,|| Grégory Vernier,‡ André Ménez,|| Daniel Gillet,*,|| Vincent Forge,*,‡ and Alexandre Chenal*,||,⊥

CEA, DSV, Département Réponse et Dynamique Cellulaires, Biophysique Moléculaire et Cellulaire, UMR 5090, 17 rue des Martyrs, 38054 Grenoble cedex 9, France, and CEA, DSV, Département d'Ingénierie et d'Etudes des Protéines, 91191 Gif sur Yvette cedex, France

Received November 16, 2006; Revised Manuscript Received December 18, 2006

ABSTRACT: During intoxication of a cell, the translocation (T) domain of the diphtheria toxin helps the passage of the catalytic domain across the membrane of the endosome into the cytoplasm. We have investigated the behavior of the N-terminal region of the T domain during the successive steps of its interaction with membranes at acidic pH using tryptophan fluorescence, its quenching by brominated lipids, and trypsin digestion. The change in the environment of this region was monitored using mutant W281F carrying a single native tryptophan at position 206 at the tip of helix TH1. The intrinsic propensity to interact with the membrane of each helix of the N-terminus of the T domain, TH1, TH2, TH3, and TH4, was also studied using synthetic peptides. We showed the N-terminal region of the T domain was not involved in the binding of the domain to the membrane, which occurred at pH 6 mainly through hydrophobic effects. At that stage of the interaction, the N-terminal region remained strongly solvated. Further acidification eliminated repulsive electrostatic interactions between this region and the membrane, allowing its penetration into the membrane by attractive electrostatic interactions and hydrophobic effects. The peptide study indicated the nature of forces contributing to membrane penetration. Overall, the data suggested that the acidic pH found in the endosome not only triggers the formation of the molten globule state of the T domain required for membrane interaction but also governs a progressive penetration of the N-terminal part of the T domain in the membrane. We propose that these physicochemical properties are necessary for the translocation of the catalytic domain.

Amphitropic proteins are proteins evolving between a soluble state and membrane-bound states to achieve their function (*1*, *2*). They are implicated in many key biological processes, such as apoptosis (*3*), gluconeogenesis (*4*), neuronal maturation (*5*), transport of hydrophobic molecules (*6*), chaperoning of proteins and lipid membranes (*7*), membrane dynamics (*8*), lipid homeostasis (*9*), endocytosis (*10*), cell signaling (*11*), cell division (*12*), DNA replication (*13*), and bacterial virulence (*14*). Understanding the physicochemical properties supporting the amphitropic behavior of these proteins is essential to understanding their mechanism of action, exploiting their properties for biotechnological applications, and modulating their function for therapy. In some cases, membrane insertion of these proteins was found to be related to hydrophobic effects and to a balance of electrostatic attractions and repulsions between charged residues of proteins and phospholipids (*4*, *9*, *15*−*17*).

Bacterial toxins of the AB_{RT} type (*18*), of which diphtheria toxin is one, act by injecting inside the cytoplasm of intoxicated cells a toxic, catalytic domain. This involves the participation of a translocation (T) domain, which has the characteristics of an amphitropic protein. The membrane insertion mechanism of the diphtheria toxin T domain[1] is one of the most documented among bacterial toxins (*19*). This T domain is composed of 10 α-helices named TH1−TH9 and TH5′, organized in a globular shape (*20*) (Figure 1). The hydrophobic helices TH8 and TH9 (Figure 1, colored red) are sandwiched by two layers of amphiphilic helices,

†This work was supported by the Commissariat à l'Energie Atomique (Grant "Signalization and membrane transport"), the CNRS, and Grant ACI Microbiologie MIC0325 from FNS.

* To whom correspondence should be addressed. D.G.: Département d'Ingénierie et d'Etudes des Protéines, CEA-Saclay, 91191 Gif sur Yvette cedex, France; telephone, (33) 1 69 08 76 46; fax, (33) 1 69 08 94 30; e-mail, daniel.gillet@cea.fr. V.F.: Biophysique Moléculaire et Cellulaire, UMR 5090, Département Réponse et Dynamique Cellulaires, CEA-Grenoble, 17 rue des Martyrs, 38054 Grenoble cedex 9, France; telephone, (33) 4 38 78 94 05; fax, (33) 4 38 78 54 87; e-mail, vincent.forge@cea.fr. A.C.: unité de Biochimie des Interactions Macromoléculaires, URA 2185, Département de Biologie Structurale et Chimie, Institut Pasteur, 25-28, rue du Dr Roux, 75724 Paris cedex 15, France; telephone, (33) 1 44 38 92 12; fax, (33) 1 40 61 30 42; e-mail, chenal@pasteur.fr.

‡ CEA, DSV, Département Réponse et Dynamique Cellulaires, Biophysique Moléculaire et Cellulaire.

§ These authors contributed equally to this work.

|| CEA, DSV, Département d'Ingénierie et d'Etudes des Protéines.

⊥ Present address: Unité de Biochimie des Interactions Macromoléculaires, URA 2185, Département de Biologie Structurale et Chimie, Institut Pasteur, 25-28, rue du Dr Roux, 75724 Paris cedex 15, France.

[1] Abbreviations: (6-7BR)-PC, 1-palmitoyl-2-stearoyl(6-7)dibromo-*sn*-glycero-3-phosphocholine; CD, circular dichroism; EPA, egg phosphatidic acid; EPC, egg phosphatidylcholine; λ_{max}, maximum emission wavelength; L:P, lipid:protein molar ratio; LUVs, large unilamellar vesicles; rFI, ratio of fluorescence intensity; T domain, translocation domain; SUVs, small unilamellar vesicles; WT, wild type.

10.1021/bi602381z CCC: $37.00
Published on Web 01/24/2007 PAGE EST: 9.5

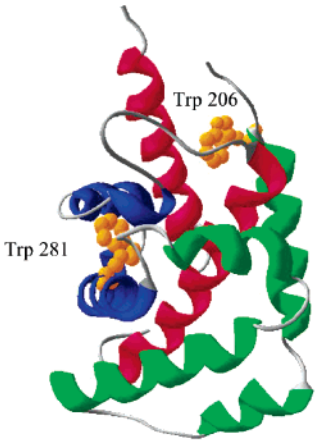

Sequence of the T-domain :

INLDWDVIRDKTKTKIESLKEHGPIKNKMSESPNKTV
SEEKAKQYLEEFHQTALEHPELSELKTVTGTNPVFA
GANYAAWAVNVAQVIDSETADNLEKTTAALSILPGI
GSVMGIADGAVHHNTEEIVAQSIALSSLMVAQAIPLVG
ELVDIGFAAYNFVESIINLFQVVHNSYNRPAYSPGHKTHA

Sequences of the peptides :

TH1 : NLDWDVIRDKTKTKIESLKEHG
TH2 : GPIKNKMSESWN
TH3 : TVSEEKAKQWLEEFHQTALE
TH4 : HPELSELKTVTGTNW

FIGURE 1: Structure,and sequences of the diphtheria toxin T domain and peptides TH1−TH4 used in this study. The structure of the T domain was from PDB entry 1F0L. Helices TH1−TH4 are colored green, TH5−TH7 blue, and TH8 and TH9 red. Trp 206 and Trp 281 are colored orange. Helices are shown in bold in the amino acid sequences. Trp residues used as fluorescent probes in the peptides are underlined. Only TH1 contains a native Trp.

TH1−TH4 (colored green) and TH5−TH7 (colored blue). During cell intoxication, the toxin is internalized into the cell endosomes. The T domain undergoes a conformational change triggered by the acidic pH found in these compartments (*19*). This triggers the penetration of T into the membrane, initiating the translocation of the catalytic domain into the cytosol (*19*). Then, the extraction of the catalytic domain from the trans side of the endosomal membrane and its release in the cytosol involve the help of cell proteins (*21*−*27*).

We showed previously that the T domain penetrates the membrane via a two-step process as the pH decreases (*28*). The protonation of several residues of the T domain destabilizes its native state, leading to the accumulation of a partially folded, molten globule state, prone to interact with membranes (*28*, *29*). During the first step, the solvent-exposed hydrophobic surfaces of the molten globule state allow binding to the membrane (*28*−*33*). This involves mainly hydrophobic effects. During the second step triggered by further acidification, a reorganization of the membrane-bound state of the T domain leads to a deeper insertion (*28*−*37*). This membrane-inserted state permeabilizes the membrane (*28*, *35*). This step involves electrostatic interactions between the T domain and anionic membranes (*28*).

We hypothesized that the second step of membrane penetration involves in particular the N-terminal helices of the T domain (*28*). We proposed that these helices shifted progressively from a position exposed to the solvent to one deeply buried within the interface of the membrane. We also proposed that this phenomenon was connected with the protonation of acidic amino acid side chains carried by these helices. The goal of this work was to test these hypotheses. A better understanding of the interaction between the N-terminal part of the T domain and the lipid bilayer is essential to describing the function of the T domain and its regulation by the pH which is required for the translocation of the catalytic domain across the endosomal membrane.

For this purpose, we produced a mutant of the T domain (W281F) carrying a single native Trp at position 206 within helix TH1 (*27*). This Trp was used as a fluorescent probe to monitor the environment of the N-terminus of T during binding to the membrane of phospholipid bilayers. To further characterize the membrane insertion process of this region, we carried out tryptophan quenching experiments using membranes containing brominated phospholipids. We also performed trypsin digestions of the membrane-inserted state of the T domain. Finally, we used four synthetic peptides corresponding to the sequence of helices TH1−TH4 composing the N-terminal region of the T domain. The results allowed the description of the successive steps followed by the N-terminal region of the T domain during its membrane insertion process. They showed also the physicochemical properties of the different helices forming this region and the nature of the interactions that are involved.

MATERIALS AND METHODS

Materials. All reagents used were of the highest purity. Fmoc-protected amino acids, Rink Amide Resin, and HBTU were purchased from Novabiochem (France Biochem, Meudon, France). The lipids, egg phosphatidylcholine (EPC, reference 830051), egg phosphatidic acid (EPA, reference 830101), and the brominated lipids (6-7BR)-PC [16:0−18:0(6-7BR)-PC, 1-palmitoyl-2-stearoyl(6−7)dibromo-*sn*-glycero-3-phosphocholine, reference 850480C] and (9-10BR)-PC [16:0−18:0(9-10BR)-PC, 1-palmitoyl-2-stearoyl(9−10)dibromo-*sn*-glycero-3-phosphocholine, reference 850481C] were purchased from Avanti Polar Lipids (Alabaster, AL). Trypsin (formally TPCK-treated trypsin, reference T-1426) and AEBSF were from Sigma (Saint-Quentin Fallavier, France).

Recombinant Proteins. The production of the recombinant T domain containing the C201S mutation (native diphtheria toxin numbering) and termed WT has been described previously (*28*). The W281F mutation was introduced by site-directed mutagenesis and the sequence checked by DNA sequencing. Purification of the recombinant proteins has been described previously (*28*). Briefly, after extraction, the soluble fraction of proteins was subjected to immobilized nickel affinity chromatography, size exclusion chromatography, and ion exchange chromatography. The purification buffer was finally exchanged with NH_4HCO_3 on a G25SF column, prior to lyophilization. The proteins were analyzed by SDS−PAGE, Western blot analysis, N-terminal protein sequencing, and electrospray mass spectrometry. The lyophi-

lized wild-type (WT) T domain and its W281F mutant were stored at −20 °C. The molar ϵ values were 18 200 and 12 200 M^{-1} cm^{-1} for the WT and W281F T domains, respectively.

Peptides. The TH1 peptide was synthesized and purified by NeoMPS (Strasbourg, France). Peptides TH2, TH3, and TH4 were synthesized on an Advanced ChemTech 357 MPS synthesizer (Advanced Chemtech Europe, Brussels, Belgium) according to the Fmoc strategy. Peptides (N-acetylated) were deprotected and cleaved from the resin by treatment with 95% trifluoroacetic acid, 2.5% triisopropylsilane, and 2.5% distilled water. They were purified to homogeneity by reversed phase HPLC on a C18 Vydac column using an acetonitrile/trifluoroacetic acid gradient. Their quality was assessed by electrospray mass spectrometry and N-terminal sequencing. The sequences of the peptides are as follows: TH1, NLDWDVIRDKTKTKIESLKEHG; TH2, GPIKNK-MSESWN; TH3, TVSEEKAKQWLEEFHQTALE; and TH4, HPELSELKTVTGTNW. The molecular masses (MM) are 2625, 1390, 2403, and 1712 Da, respectively, and the p*K* values are 7.7, 8.6, 4.7, and 5.4, respectively; the molar ϵ at 280 nm (E_M) is 5500 M^{-1} cm^{-1} for all peptides. Only the Trp in the sequence of the TH1 peptide is native; the other Trp residues were introduced into the peptide sequences as spectroscopic probes.

Lipid Vesicles. Vesicle suspensions of anionic lipid bilayers at a lipid concentration of 10 mM were prepared in 10 mM sodium citrate/citrate buffer (pH 7) with EPC and EPA at a 9:1 molar ratio by reverse phase evaporation and filtration for large unilamellar vesicles (LUVs) and by sonication for small unilamellar vesicles (SUVs). In the presence of brominated lipids, the EPC:BR-PC:EPA ratio was 5:4:1; the LUVs and SUVs were prepared as described above but at 37 °C.

Preparation of Samples. The proteins were diluted in 5 mM citrate buffer at the indicated pH. The peptides were diluted in 10 mM citrate buffer for fluorescence experiments and 4 mM citrate buffer for circular dichroism experiments. In partitioning experiments, proteins or peptides and anionic SUVs or LUVs were mixed at L:P molar ratios ranging from 0 to 1000 and incubated for 2 h at 22 °C. To study the interaction of proteins or peptides with membranes as a function of pH, proteins and LUVs were mixed at an L:P of 500 and peptides and SUV were mixed at an L:P of 1000. Samples were incubated for 2 h at 22 °C and 2 h at 37 °C when brominated lipids were used, before experiments. pH values were always measured afterward. A stock solution of 5 M NaCl was used for experiments performed in the presence of 200 mM NaCl.

CD Spectropolarimetry. For proteins, CD experiments were performed on a CD6 spectrodichrograph (Jobin-Yvon Instruments, Longjumeau, France) as described previously (*29*). The scans were recorded using a bandwidth of 2 nm and an integration time of 1 s at a scan rate of 0.5 nm/s. Each spectrum is the average of 20 scans and 10 scans for near-UV and far-UV measurements, respectively. Protein concentrations were 20 and 5 μM for near-UV and far-UV measurements, respectively. The spectra were corrected for the blank, and a smoothing algorithm was used with the minimum filter in the CD6 software (CDMax, filter 5).

For peptides, CD experiments were performed on a J-810 spectropolarimeter (Jasco, Tokyo, Japan) with a 1 mm path length quartz cell, using a bandwidth of 4 nm, an integration time of 1 s, and a scan rate of 0.8 nm/s. Each spectrum is the average of 40 scans. The peptide concentration was 20 μM.

Fluorescence Spectroscopy. For proteins, measurements were performed with an FP-750 spectrofluorimeter (Jasco) in a thermostated cell holder, using a 1 cm path length quartz cell, as described previously (*29*). A bandwidth of 5 nm was used for both excitation and emission beams. The excitation wavelength was fixed at 292 nm. The emission spectra were recorded from 300 to 400 nm at a scan rate of 125 nm/min. The maximum emission wavelength (λ_{max}) and fluorescence intensity ratios at 360 nm to 320 nm (rFI 360/320) represent the average of three values obtained from emission spectra that were corrected for blank measurements. The protein concentration was 1 μM.

For peptides, measurements were taken using a Jasco FP-6500 spectrofluorimeter using a 1 cm path length quartz cell. The bandwidth was 5 nm for both excitation and emission beams. The excitation wavelength was fixed at 280 nm, and emission spectra were recorded from 300 to 400 nm at a scan rate of 100 nm/min. λ_{max} represents the average of three values obtained from emission spectra corrected for blank measurements. The peptide concentration was 2 μM.

With regard to the experiments performed in the presence of brominated lipids, the fluorimeter was thermostated at 37 °C. The experiments were carried out on a photon technology international QM-4/2005 SE spectrofluorimeter using a 1 cm path length quartz cell, at 37 °C. A bandwidth of 5 nm was used for both excitation and emission beams. The excitation wavelength was fixed at 292 nm, and emission spectra were recorded from 300 to 400 nm.

Binding of Proteins to LUVs Studied by Centrifugation. LUVs and proteins were incubated for 2 h at 22 °C in 4 mL of 5 mM citrate buffer. After fluorescence measurements, each sample was centrifuged in an L-70 ultracentrifuge (Beckman, Roissy, France) using a Ti 70.1 rotor at 60 000 rpm for 20 min at 22 °C. The fraction of bound proteins was determined as $(F_0 - F)/F_0$, where F_0 is the fluorescence intensity of the sample before centrifugation and in the absence of LUVs (i.e., before the addition of LUVs) and F is the intensity of the supernatant after centrifugation in the presence of LUVs.

Proteolytic Cleavage Experiments. The T domain (10 μM) was incubated in the absence or presence of LUV at an L:P of 500 in 5 mM citrate buffer at pH 4 in the presence or absence of 200 mM NaCl. Trypsin was added at a final concentration of 0.1 μM. Such a T domain:trypsin ratio was necessary due to the low proteolytic activity of the enzyme at acidic pH. Samples were incubated at 22 °C for the indicated time, and proteolysis was blocked by the addition of AEBSF at a final concentration of 200 μM; samples were immediately frozen in liquid nitrogen and stored at −20 °C. Protein cleavage was then analyzed by SDS−PAGE on a 15% gel followed by electro-transfer on a PVDF membrane and Coomassie blue staining. Stained bands corresponding to cleaved protein fragments were cut out from the membrane and sequenced by automated N-terminal Edman degradation.

RESULTS

The T domain carries two Trp residues, one at position 206 on helix TH1 and the other at position 281 on helix

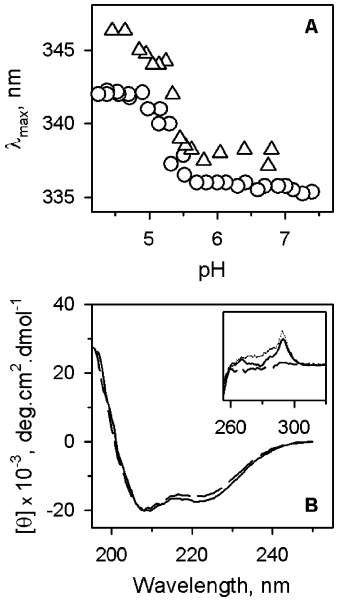

FIGURE 2: Effect of pH on the conformation of W281F and the WT T domain in solution. (A) λ_{max} of Trp fluorescence of W281F (△) and WT T domain (○) as a function of pH. (B) Far-UV CD spectra obtained for W281F at pH 7 (—) and pH 4 (− − −). The inset shows the near-UV CD spectra recorded under the same pH conditions for W281F and at pH 7 for WT T (thin line).

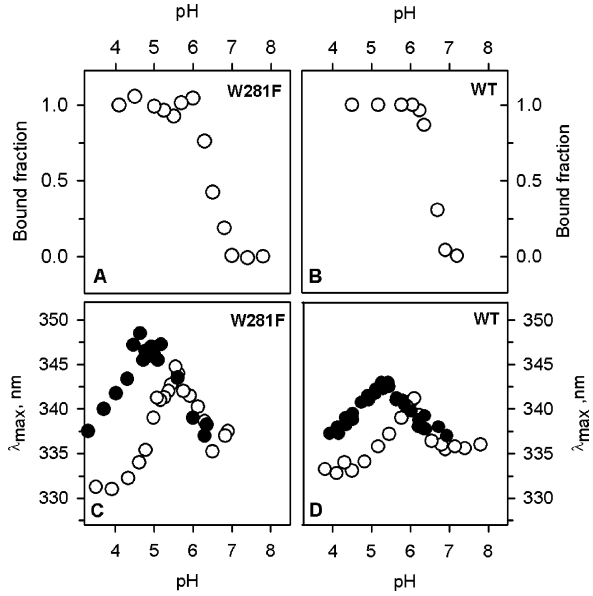

FIGURE 3: Effect of pH and NaCl on the interaction with membranes and conformation of W281F and WT T domain. (A and B) Partition of W281F and the WT T domain between buffer and anionic LUVs as a function of pH studied by ultracentrifugation. (C and D) Trp fluorescence of W281F and the WT T domain as a function of pH in the presence of anionic LUVs at an L:P of 500. Measurements were taken in the absence (○) and presence (●) of 200 mM NaCl. The protein concentration was 1 μM.

TH5 (Figure 1). To monitor the conformational changes affecting the N-terminal part of the T domain both in solution and interacting with membranes, we constructed the single Trp mutant W281F. The remaining Trp 206 was used as a fluorescent probe monitoring the changes in the environment of helix TH1. We studied whether the W281F mutation affected the conformational change of the T domain induced at acidic pH, which is responsible for membrane binding. The Trp fluorescence of both proteins, the W281F mutant [Figure 2A (△)] and the wild-type (WT) T domain [Figure 2A (○)], was measured as a function of pH. As the pH decreases, a shift of λ_{max} toward red wavelengths was observed for both proteins. This reflected a partial exposure of their Trp to the aqueous phase at acidic pH. The λ_{max} of W281F was close to that of the WT T domain at neutral pH (338 vs 336 $\pm$ 0.5 nm) and higher at acidic pH (346 vs 342 $\pm$ 0.5 nm). We then checked that for W281F this pH-induced transition was related to the adoption of a molten globule state as shown previously for the WT T domain (*28*, *29*). Far-UV CD spectra showed that both proteins exhibited a similar α-helical content at pH 7 and 4 [Figure 2B for W281F, not shown for WT (*28*)]. At neutral pH, the two proteins also had similar near-UV CD spectra and the sharp dichroic band at 292 nm, assigned to a Lb band of Trp constrained in a chiral environment within the tertiary structure of the T domain, disappeared at acidic pH (Figure 2B, inset). This revealed an increase in mobility of Trp 206 at acidic pH.

We studied the binding of W281F to membranes as a function of pH. The WT T domain was used for comparison. The physical partition of both proteins between the aqueous phase and the membrane phase of a suspension of LUVs occurred between pH 7 and 6, all molecules being bound to the LUVs at pH 6 (Figure 3A,B). As described previously (*28*), the pH dependence of the binding was cooperative, with Hill coefficients around 3. The Trp fluorescence of W281F (Figure 3C) revealed that the interaction with the membrane took place in two steps, as for the WT T domain (Figure 3D). These experiments were performed in the absence and presence of NaCl because we showed previously that NaCl influenced this process for the WT T domain (*28*).

During the first step, from pH 7 to 5.8, the λ_{max} of the fluorescence of W281F increased from about 338 to 345 nm [Figure 3C (○)], overlapping the binding monitored in centrifugation experiments (Figure 3A). This indicated progressive exposure of Trp 206 to a polar environment upon binding to the membrane. In the presence of NaCl, the first transition was extended to pH 5, the λ_{max} reaching 347 nm (instead of 345 nm in the absence of NaCl) in the case of W281F [Figure 3C (●)]. Then during the second step, from pH 5.8 to 4 and in the absence of NaCl, the λ_{max} dropped from 345 to 331 nm [Figure 3C (○)]. This suggested that Trp 206 reached a hydrophobic environment while the protein was already bound to the membrane. At acidic pH, both proteins induced the leakage of dye (pyranine) encapsulated in LUVs (data not shown). The presence of NaCl shifted the second transition, which occurred at a pH more acidic by more than 1 pH unit. The WT T domain exhibited the same behavior, except that the amplitude of the fluorescence transition was lower due to the measurement of the fluorescence of both Trp residues. The NaCl effects shown here were larger than those described in our previous article (*28*) because the NaCl concentration was higher (200 mM instead of 100 mM).

To better characterize the environment of the N-terminal region of the T domain during the pH-dependent membrane interaction process, we measured the quenching of the Trp fluorescence of the W281F T domain by brominated phospholipids (*38*−*42*). We used lipids with bromines covalently bound at positions C6 and C7 of the acyl chains, close to the interfacial region of the membrane [(6-7BR)-PC]. We

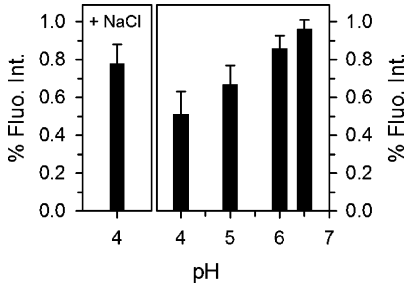

FIGURE 4: Quenching of the W281F T domain Trp fluorescence by brominated phospholipids. The pH dependency of Trp fluorescence quenching is measured in the presence of (6-7BR)-PC. The experiments were conducted with 500 μM lipids and 1 μM T, in the absence (right) and presence (left) of 200 mM NaCl.

performed the experiments at pH 7, 6, 5, and 4, in the presence and absence of NaCl. The results are expressed as the relative quenching efficiency of the initial Trp fluorescence by the brominated lipids (Figure 4): the lower the value, the closer the quencher from the Trp. During the membrane binding step, between pH 6.5 and 6, the quenching is low (up to 10%) (Figure 4, right). This suggests Trp 206 remained far from the quenchers while T was already bound to the membrane (Figure 3A). As the pH further decreases between pH 5 and 4, the quenching strongly increased, up to 50−60% (Figure 4). This indicated that the apolar milieu reached by the Trp (λ_{max}, 331 nm in Figure 3C) was the hydrophobic core of the lipid bilayer. At pH 4, the quenching was weaker in the presence of NaCl than in its absence (Figure 4, left). This indicated that the N-terminal region was less inserted in the membrane and located in a more polar environment in the presence of NaCl than in its absence. This corroborated the red shift of the λ_{max} of Trp fluorescence we measured with the addition of NaCl (Figure 3C, pH 4). Altogether, we showed that Trp 206 was exposed to the solvent in the membrane-bound state, while it penetrated the membrane during the second step of the membrane interaction process. This second step is sensitive to electrostatic interactions between the charges of the N-terminal region of T and lipid head groups.

To further describe the sensitivity of the N-terminal region of T to NaCl during interaction with the membrane, we performed a lipid titration at pH 4. We monitored the physical partition of W281F between the buffer and the membrane in a suspension of LUV at pH 4 as a function of lipid concentration (Figure 5A). Again, the WT T domain was used for comparison (Figure 5B). Both proteins were fully bound to the LUV at an L:P of 100. Binding was not influenced by the presence of NaCl. This suggested that, as already observed for the pH dependence of the interaction with the membrane, binding involved mainly hydrophobic effects. The Trp fluorescence of W281F in the presence of membranes (Figure 5C) revealed that the interaction with the membrane took place in two steps, as for the WT T domain (Figure 5D). But again, the modification of the fluorescence signal of W281F was much stronger, showing that Trp 206 was the main contributor to the signal of the WT T domain in the second transition. For these experiments, the ratio between the intensities at 360 and 320 nm (rFI) was used instead of the λ_{max} because this ratio could monitor the spectrum shift with a higher sensitivity (Figure 5C,D). The value of rFI decreased as the fluorescence spectrum

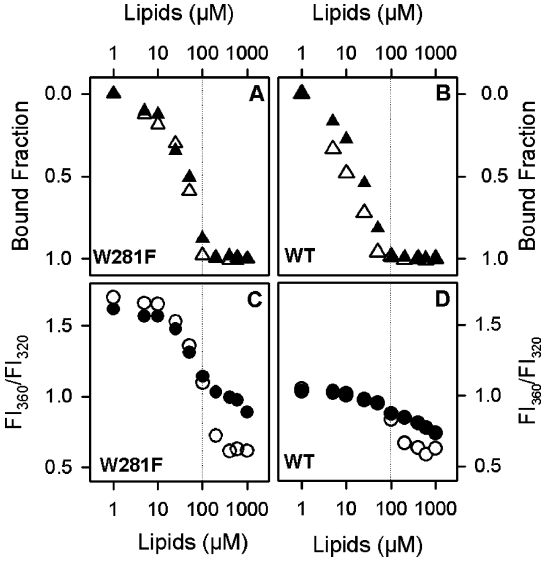

FIGURE 5: Interaction of W281F and the WT T domain with membranes at acidic pH as a function of lipid concentration. (A and B) Partition of W281F and the WT T domain between buffer and anionic LUVs at pH 4 as a function of lipid concentration studied by ultracentrifugation. Measurements were taken in the absence (△) and presence (▲) of 200 mM NaCl. (C and D) Trp fluorescence of W281F and the WT T domain at pH 4 as a function of lipid (LUV) concentration. Measurements were taken in the absence (○) and presence (●) of 200 mM NaCl. The protein concentration was 1 μM. FI_{360}/FI_{320} is the ratio of the fluorescence intensity at 360 nm to that at 320 nm.

shifted toward shorter wavelengths, i.e., as the Trp penetrated a hydrophobic environment. At pH 4 and in the absence of LUV, the λ_{max} of W281F was around 347 nm (Figure 2A). This gave an rFI value of around 1.7 (Figure 5C). In the case of the WT T domain, the λ_{max} was around 342 nm (Figure 2A), giving a rFI of around 1.0 (Figure 5D). When both proteins bound tightly to the lipid bilayer, the λ_{max} was around 332 nm (Figure 3C,D) and the rFI was then around 0.6 (Figure 5C,D). In the absence of NaCl, only one transition was observed, the Trp going from a polar to an apolar environment. However, in the presence of 200 mM NaCl, two steps could be distinguished. A first transition occurred up to an L:P of 100, and the environment of Trp 206 shifted progressively from polar to apolar as the L:P increased. This step was not affected by NaCl, and it paralleled the binding monitored in the partition experiments (Figure 5A,B). For L:P of >100, once all molecules were bound, a second transition occurred, Trp 206 further gaining a more hydrophobic environment [Figure 5C (○)]. In contrast to the first transition, NaCl inhibited this second transition and made it detectable [Figure 5C (●)]. This showed that it was controlled by electrostatic interactions.

Trypsin cleaves polypeptides after lysine and arginine side chains (*43*). Interestingly, the T domain contains one arginine and 11 lysine residues within helices TH1−TH4 and one lysine in helix TH6 (Figures 1 and 6). Hence, the sensitivity of the T domain to trypsin digestion was studied as a marker of the accessibility of its N-terminal region. Experiments were conducted at pH 4, in solution and in the presence of membranes, in the presence and absence of NaCl. The concentration of trypsin was adjusted to make the proteolysis possible despite the acidic pH (see Materials and Methods). With membranes, experiments were conducted at an L:P of 500, at which the structural reorganization of the T domain

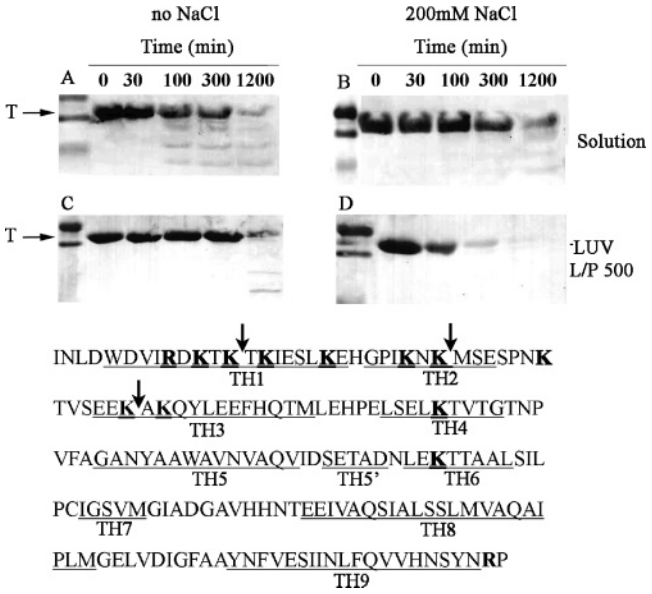

FIGURE 6: Trypsin digestion of the WT T domain at pH 4 in solution (A and B) and in interaction with anionic LUVs (C and D) in the absence (A and C) or presence (B and D) of NaCl. In the presence of membranes, the L:P was 500. Digestion times are given. The arrows over the sequence of the T domain indicate the main cleavage sites as determined by N-terminal sequencing.

in the membrane, i.e., the second step of the interaction, was fully achieved in the absence of NaCl but barely started in its presence (Figure 5C,D). The integrity of the T domain was evaluated by SDS−PAGE, and cleavage sites were identified by N-terminal sequencing of the protein fragments. Whatever the conditions that were assayed, when cleavage occurred, three main cleavage sites were found, in helices TH1−TH3 (Figure 6). In solution, the T domain was moderately sensitive to digestion. The proteolysis seemed slightly slower in the presence of NaCl. When bound to membranes, the T domain became more resistant to digestion in the absence of NaCl, i.e., when the two steps of the interaction with the membranes were completed under the conditions used for the experiment. On the other hand, in the presence of NaCl, i.e., after the first step only (the binding) was completed for an L:P value of 500, the digestion was significantly faster.

We have shown that the N-terminal region of the T domain underwent a significant structural reorganization during the process of insertion into the membrane. To examine whether the physicochemical properties of the sequences of the N-terminal helices of the T domain may play a role in the binding process, and more particularly in its pH dependence, four peptides corresponding to the helices TH1−TH4 were synthesized (Figure 1). A Trp was included in each peptide as a fluorescent probe, except for TH1, which contained the native Trp 206. We measured the fluorescence of each peptide as a function of pH in the absence and presence of anionic SUVs. No binding of the peptides to LUVs has been detected. In the absence of SUVs, the λ_{max} of each peptide remained around 354 nm whatever the pH (not shown). In the presence of SUVs, the λ_{max} of peptides TH1 [Figure 7A (○)], TH3 [Figure 7C (△)], and TH4 [Figure 7C (□)] shifted toward lower values as the pH decreased. For the three peptides, the changes occurred within similar pH ranges between pH 6 and 4. The transition was sharper in the case of TH3. This indicated that the transition for this peptide

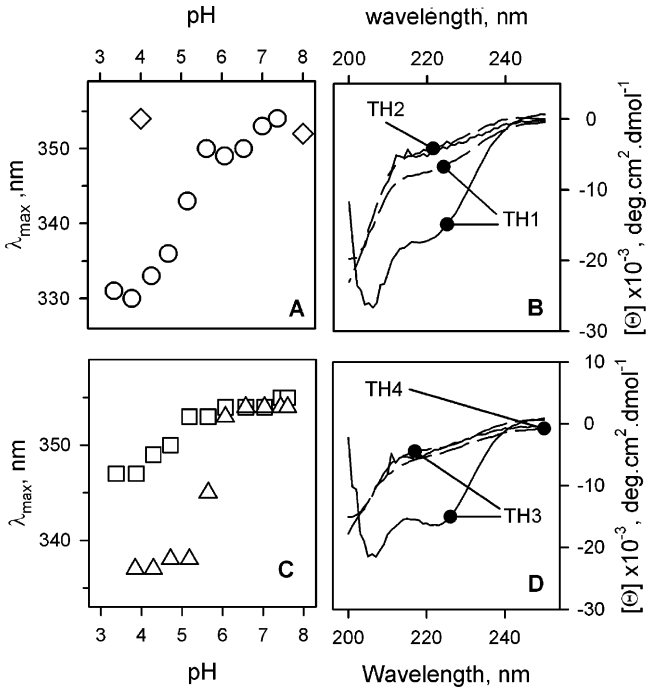

FIGURE 7: Interaction of peptides TH1−TH4 with membranes as a function of pH. (A and C) The λ_{max} of Trp fluorescence of the peptides was measured as a function of pH in the presence of anionic SUVs at an L:P of 1000. Acidification did not affect the λ_{max} of the peptides in the absence of SUVs (not shown): TH1 (○), TH2 (◇), TH3 (△), and TH4 (□). (B and D) Far-UV CD spectra obtained for the peptides at pH 4 in the absence (− − −) or presence (—) of anionic SUVs.

was cooperative, probably because of oligomerization upon binding to the lipid bilayer. Below pH 4, the λ_{max} of these peptides reached 330, 337, and 347 nm, respectively. This indicated that the Trp residues of these peptides were progressively surrounded by an apolar environment, suggesting binding of the peptides and penetration into the lipid bilayer. In contrast, the λ_{max} of TH2 remained constant [Figure 7A (◇)]. The fluorescence quenching by brominated lipids was measured to determine if the blue shift of the fluorescence spectra was due to the penetration of the peptides within the hydrophobic core of the membrane. The quenching observed for TH1 and TH3 was 42 and 48%, respectively. In parallel, far-UV CD spectra of the peptides were recorded at pH 4, in the absence and presence of SUVs (Figure 7B,D). All peptides were poorly structured in the absence of membranes [Figure 7B,D (− − −)]. The presence of NaCl had no effect on the secondary structure content of the peptides in solution whatever the pH (data not shown). Interestingly, peptides TH1 and TH3 generated significant signals of α-helices at acidic pH in the presence of SUVs [Figure 7B,D (—)]. This suggested that binding of peptides TH1 and TH3 to the SUVs triggered their folding into α-helices.

We then investigated the effect of ionic strength on the interaction of the peptides with the membrane. For this purpose, we monitored the fluorescence of each peptide as a function of phospholipid concentration, at pH 8 and 4, in the absence and presence of NaCl (Figure 8). At pH 8, the λ_{max} of the fluorescence of the peptides was moderately affected or not at all as L:P increased [Figure 8 (△)]. In contrast, at pH 4 and in the absence of NaCl, the λ_{max} of peptides TH1 and TH3 and to a lesser extent that of TH4

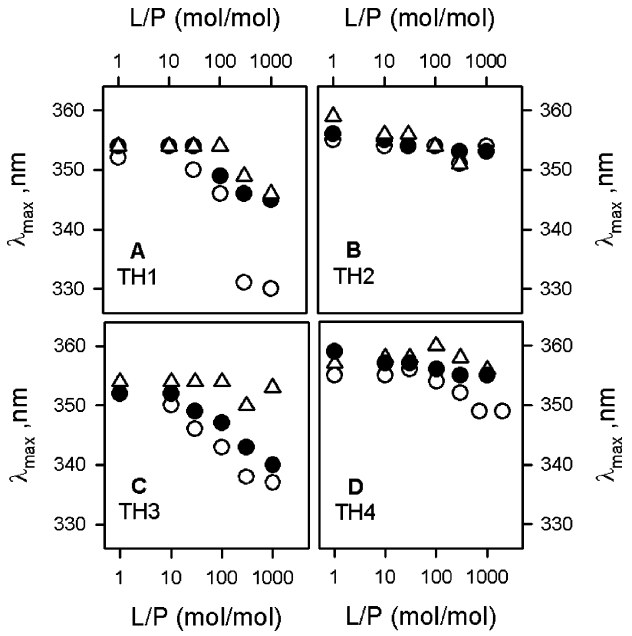

FIGURE 8: Interaction of peptides TH1−TH4 with membranes as a function of lipid concentration and NaCl at pH 8 and 4. The λ_{max} of Trp fluorescence of the peptides was measured in the presence of increasing concentrations of lipids (anionic SUVs) at pH 8 (△) or pH 4 in the absence (○) or presence (●) of 200 mM NaCl. The peptide concentration was 2 μM.

shifted toward lower values [Figure 8 (○)]. This was expected from the previous experiment (Figure 7A). Maximum shifts were reached around an L:P of 300−1000. Interestingly, NaCl inhibited these shifts for peptides TH1 and TH4 but had practically no effect for TH3 (Figure 8). Again, the fluorescence of TH2 was not affected under any of the conditions that were assayed. Collectively, the data strongly suggest that the isolated peptides TH1, TH3, and to a lesser extent TH4 have the intrinsic propensity to bind to membranes at acidic pH but not TH2. In addition, binding induced the folding of TH1 and TH3 into α-helices. The fact that binding of TH1 and TH4 was inhibited by NaCl showed that electrostatic interactions were involved. In contrast, binding of TH3 was not, which suggested that hydrophobic effects were preponderant in that case. Noteworthy is the fact that the pH dependences of the interactions of the three peptides TH1, TH3, and TH4 with membranes were similar to that of the second transition detected with the whole T domain.

DISCUSSION

In a previous article, we have described two steps in the pH-dependent interaction between the T domain and the membrane (*28*). The binding to the membrane occurs in a first step and involves mainly hydrophobic forces. The functional state of the T domain appears in a second step, at more acidic pH, and induces a permeabilization of the membrane. The sensitivity of this second step to the presence of NaCl shows that electrostatic interactions between the T domain and the lipid bilayer interface are required. On the basis of our observations, we have proposed that the N-terminal region of the T domain, which is made of amphiphilic α-helices, plays a key role in the second step of the interaction, i.e., the formation of the functional state of the T domain. We have also proposed that the interactions between the amphiphilic α-helices of the T domain and the acidic phospholipid head groups become attractive due to the protonation of the side chains of acidic amino acid residues upon acidification of the environment. This phenomenon allows a tighter interaction between the N-terminal region and the membrane interface. These hypotheses have been tested here. We have produced a W281F T domain harboring a unique and native Trp 206, located at the N-terminal extremity of TH1. This Trp has been used as a reporter of the conformational changes undergone by this region of the protein. We also investigated the intrinsic propensity of the amino acid sequences of the four N-terminal helices to interact with membranes using peptides.

In solution, our results showed that the W281F mutant and the WT T domain displayed the same pH-dependent conformational changes, leading to a molten globule state (Figure 2), as previously characterized for the WT T domain (*28*): the secondary structures remained nativelike, while the tertiary structure was lost. In the presence of negatively charged membranes, both WT and W281F T domains exhibit similar behavior, the later allowing a detailed characterization of the molecular events occurring in the N-terminal part of the T domain.

From pH 8 to 6, the T domain binds to the membrane and is insensitive to NaCl as shown by partition experiments. During this process, Trp 206 becomes more exposed to a polar environment, which could be the solvent or the proximity to charged side chains of amino acids. In the membrane-bound state, at pH ∼6, Trp 206 is solvated, as revealed by its red λ_{max} and the negligible quenching of its fluorescence by brominated lipids. Hence, the acquisition of the membrane-bound state is mainly driven by hydrophobic effects between the C-terminal part of the T domain and the membrane. From pH 6 to 4, the functional, membrane-inserted state is stabilized. Our results provide direct evidence that the behavior of the N-terminal part of the T domain is crucial in this second step of the membrane interaction process. Indeed, the λ_{max} of Trp 206 experienced a marked blue shift, from 347 to 331 nm, which was concomitant with a strong quenching of Trp fluorescence by brominated lipids. This second transition is highly sensitive to the presence of NaCl, revealing the electrostatic contribution to the interaction between this region of T and the anionic lipid head groups of the membrane. Moreover, peptides TH1, TH3, and TH4 clearly exhibited pH-dependent membrane binding. Altogether, these results clearly demonstrate that once T is bound to the membrane via hydrophobic effects, its N-terminal region moves progressively from the solvent into the membrane environment. We propose these helices reach the interfacial region of the membrane.

Two steps are also observed during the interaction of the T domain with the membrane as a function of the lipid concentration at pH 4 (Figure 5). The first step (from 0 to 100 μM lipid) is monitored by partition experiments and is insensitive to the presence of NaCl (Figure 5A,B). Hence, this first step corresponds to the binding of the T domain to the lipid bilayer and is mostly driven by hydrophobic forces. Interestingly, the first step of the pH-dependent membrane interaction corresponds also to the membrane binding of T mainly through hydrophobic effects. The environment of the Trp residues is modified upon binding (Figure 5C,D, vertical dotted line). However, at this stage (pH 4 and 100 μM lipid),

Trp 206 is located in a less polar environment (λ_{max} = 337 nm and rFI = 1.1; Figure 5C, vertical dotted line) than in the case of the interaction monitored as a function of pH (λ_{max} = 345 nm; Figure 3C). We propose the following explanation for the difference in polarity surrounding Trp 206 once T is bound to the membrane at both pHs. When the membrane binding of T as a function of lipid concentration is monitored at pH 4, electrostatic repulsions between the protonated acidic side chains of the protein and the anionic phospholipid head groups are abolished. This is not the case when binding is monitored as a function of pH (in the presence of 500 μM lipid) because the first step is completed around pH 6, the pH at which acidic side chains are still negatively charged. This shows that the electrostatic interactions have an effect on the conformation of the T domain upon binding, although they are not required at this stage of the interaction. In contrast to the first step, the second step detected when monitoring the interaction as a function of lipid concentration is inhibited in the presence of NaCl; i.e., electrostatic attractions between the basic side chains of the protein and the acidic phospholipids are required. The two steps are clearly distinguished in the presence of NaCl. This is particularly true in the case of W281F (Figure 5C). The value of λ_{max} and the quenching of Trp fluorescence by brominated lipids both indicate that the Trp residues are located inside the membrane.

The changes in λ_{max} detected for W281F when monitoring the interaction of the protein with the bilayer as a function of pH or as a function of lipid concentration are similar to those reported for the WT T domain. The remaining Trp of W281F, at the tip of helix TH1, is located in a polar environment upon binding to the lipid bilayer and then penetrates progressively into an apolar milieu during the second step of the interaction, leading to the functional state of the T domain. This suggests that the environment of the N-terminal region of the T domain changes dramatically during the interaction with the membrane. At an L:P of 500 and at pH 4 (Figure 5), the domain is stabilized in the intermediate state (between the first and second step) in the presence of NaCl while it is in the functional state in the absence of salt (the second step is completed). This allowed the investigation of the accessibility of the N-terminal part of the T domain to proteolysis (Figure 6). This part of the protein is accessible to the proteases in the intermediate state of the interaction, and it becomes protected against proteolysis in the functional state. Therefore, not only TH1 but the whole amphiphilic N-terminal part (TH1−TH4) becomes less accessible to the solvent during the second step of the interaction, whereas it is quite accessible after the binding.

The results support the hypothesis that, during the second step, the interaction between the N-terminal region of the T domain and the lipid bilayer interface is controlled by hydrophobic forces together with electrostatic interactions, both repulsive and attractive (*28*). According to our hypothesis, during the second step, as the pH decreases, the acidic side chains of the N-terminal amphiphilic helices are protonated and the repulsive interactions with the acidic phospholipids are abolished. Then, only the favorable interactions, the hydrophobic and the electrostatic attraction between the basic side chains and the acidic phospholipids, remain, and the interactions between the N-terminal region of the T domain and the lipid bilayer interface are tighter. To provide further evidence of this proposition, we have investigated the interactions of peptides corresponding to the amphiphilic helices of the N-terminal region (TH1−TH4) (Figure 1).

Among the four peptides investigated here, TH1 and TH3 exhibit tight interaction with SUVs, TH4 exhibits a weak interaction detected by fluorescence, and TH2 exhibits no interaction (Figures 7 and 8). We noticed membrane interaction is stronger in the presence of SUVs than in the presence of LUVs. The high membrane curvature of SUVs induces an asymmetric distribution of lipids between the two leaflets (*44*), resulting in a smaller order parameter and a weaker lateral pressure of lipids in the outer leaflet of the vesicle (*45*−*52*). As a consequence, the first hydrocarbon groups following the ester bond of lipids in SUVs are more exposed to the membrane interface than in LUVs, and the hydrophobic interactions are facilitated (*53*). These effects explain the binding of the peptides to SUVs rather than to LUVs.

Whatever the pH, in the absence and presence of NaCl, the four peptides adopt random coil conformations (Figure 7B,D and not shown). TH1 and TH3 become α-helical at acidic pH due to their binding to lipid vesicles. The formation of hydrogen bonds is concomitant with the interaction of the peptides with the lipid bilayer in minimizing the energy of the system and leads to the formation of α-helices (*54*, *55*). The interaction of TH1 and TH3 with the lipid vesicles occurs in a pH range similar to that of the whole T domain, i.e., between pH 6 and 4 (Figure 7A,C). This is also true for the weak interaction of TH4 (Figure 7C). As described for other peptides, this pH dependence is due to the protonation of the acidic side chains (*56*−*58*). Both TH1 and TH3 contain five acidic side chains (Asp or Glu) (Figure 1). In the presence of NaCl, the interaction of TH1 with the lipid vesicles is inhibited while that of TH3 remains mostly unaltered (Figure 8A,C), suggesting that the electrostatic interactions are less preponderant in the case of TH3. This can be related to the number of basic amino acids (Arg or Lys) present in the peptide. Peptide TH1 contains five basic side chains, while peptide TH3 has only two of those. It is likely that, upon protonation of its acidic side chains, TH3 becomes hydrophobic enough for the interaction and the attractive interactions between the basic side chains and the acidic phospholipids are not essential. In the case of peptide TH1, these interactions are required, which is the case for the formation of the functional state of the T domain. These results provide direct evidence that the four peptides behave differently. Nevertheless, they also clearly show that the N-terminal sequence of T has an intrinsic propensity to interact with anionic lipid bilayers in a pH-dependent manner.

Overall, our results highlight the role of the amphiphilic N-terminal region of the T domain through the membrane insertion process. The formation of the functional state is related to a change in the location of the amphiphilic helices, from a solvent-exposed location in the membrane-bound state at pH 6 to an apolar environment in the membrane-inserted state at pH 4. The interaction of these helices with the membrane is controlled by the balance between attractive and repulsive electrostatic interactions. As shown here, the binding of these amphiphilic α-helices depends on the protonation of their acidic side chains. The interplay between the pH dependence of electrostatic repulsion between the acidic side chains and the acidic phospholipid head groups

and the electrostatic attraction due to the basic side chains allows a tight control by the pH of the formation of the functional state of the T domain. It also provides sensitivity of the translocation of this part of the domain to the pH gradient across the endosome membrane and hence facilitates the translocation of the catalytic domain of the toxin.

ACKNOWLEDGMENT

We thank Robert Thai for N-terminal protein sequencing and Mélanie Leleu and Bernard Maillère for peptide synthesis.

REFERENCES

1. Mosior, M., and Epand, R. M. (1997) Protein kinase C: An example of a calcium-regulated protein binding to membranes, *Mol. Membr. Biol. 14*, 65−70.
2. Muller, G., and Bandlow, W. (1989) An amphitropic cAMP-binding protein in yeast mitochondria. 1. Synergistic control of the intramitochondrial location by calcium and phospholipids, *Biochemistry 28*, 9957−9967.
3. Cheng, E. H., Levine, B., Boise, L. H., Thompson, C. B., and Hardwick, J. M. (1996) Bax-independent inhibition of apoptosis by Bcl-XL, *Nature 379*, 554−556.
4. Neve, E. P., Hidestrand, M., and Ingelman-Sundberg, M. (2003) Identification of sequences responsible for intracellular targeting and membrane binding of rat CYP2E1 in yeast, *Biochemistry 42*, 14566−14575.
5. Mosevitsky, M. I. (2005) Nerve ending "signal" proteins GAP-43, MARCKS, and BASP1, *Int. Rev. Cytol. 245*, 245−325.
6. Bose, H. S., Whittal, R. M., Baldwin, M. A., and Miller, W. L. (1999) The active form of the steroidogenic acute regulatory protein, StAR, appears to be a molten globule, *Proc. Natl. Acad. Sci. U.S.A. 96*, 7250−7255.
7. Torok, Z., Goloubinoff, P., Horvath, I., Tsvetkova, N. M., Glatz, A., Balogh, G., et al. (2001) Synechocystis HSP17 is an amphitropic protein that stabilizes heat-stressed membranes and binds denatured proteins for subsequent chaperone-mediated refolding, *Proc. Natl. Acad. Sci. U.S.A. 98*, 3098−3103.
8. Richter, R. P., Him, J. L., Tessier, B., Tessier, C., and Brisson, A. R. (2005) On the kinetics of adsorption and two-dimensional self-assembly of annexin A5 on supported lipid bilayers, *Biophys. J. 89*, 3372−3385.
9. Johnson, J. E., Xie, M., Singh, L. M., Edge, R., and Cornell, R. B. (2003) Both acidic and basic amino acids in an amphitropic enzyme, CTP:phosphocholine cytidylyltransferase, dictate its selectivity for anionic membranes, *J. Biol. Chem. 278*, 514−522.
10. Ford, M. G., Mills, I. G., Peter, B. J., Vallis, Y., Praefcke, G. J., Evans, P. R., et al. (2002) Curvature of clathrin-coated pits driven by epsin, *Nature 419*, 361−366.
11. Del Boca, M., Caputto, B. L., Maggio, B., and Borioli, G. A. (2005) c-Jun interacts with phospholipids and c-Fos at the interface, *J. Colloid Interface Sci. 287*, 80−84.
12. Mileykovskaya, E., and Dowhan, W. (2005) Role of membrane lipids in bacterial division-site selection, *Curr. Opin. Microbiol. 8*, 135−142.
13. Sekimizu, K., and Kornberg, A. (1988) Cardiolipin activation of dnaA protein, the initiation protein of replication in *Escherichia coli*, *J. Biol. Chem. 263*, 7131−7135.
14. Zakharov, S. D., and Cramer, W. A. (2002) Colicin crystal structures: Pathways and mechanisms for colicin insertion into membranes, *Biochim. Biophys. Acta 1565*, 333−346.
15. Dowhan, W., Mileykovskaya, E., and Bogdanov, M. (2004) Diversity and versatility of lipid-protein interactions revealed by molecular genetic approaches, *Biochim. Biophys. Acta 1666*, 19−39.
16. Kim, J., Shishido, T., Jiang, X., Aderem, A., and McLaughlin, S. (1994) Phosphorylation, high ionic strength, and calmodulin reverse the binding of MARCKS to phospholipid vesicles, *J. Biol. Chem. 269*, 28214−28219.
17. Chenal, A., Vernier, G., Savarin, P., Bushmarina, N. A., Geze, A., Guillain, F., et al. (2005) Conformational states and thermodynamics of α-lactalbumin bound to membranes: A case study of the effects of pH, calcium, lipid membrane curvature and charge, *J. Mol. Biol. 349*, 890−905.
18. Menetrey, J., Gillet, D., and Menez, A. (2005) Structural features common to intracellularly acting toxins from bacteria, *Toxicon 45*, 129−137.
19. Chenal, A., Nizard, P., and Gillet, D. (2002) Structure and function of diphtheria toxin: From pathology to engineering, *J. Toxicol., Toxin Rev. 21*, 321−359.
20. Bennett, M. J., and Eisenberg, D. (1994) Refined structure of monomeric diphtheria toxin at 2.3 Å resolution, *Protein Sci. 3*, 1464−1475.
21. Lemichez, E., Bomsel, M., Devilliers, G., vanderSpek, J., Murphy, J. R., Lukianov, E. V., Olsnes, S., and Boquet, P. (1997) Membrane translocation of diphtheria toxin fragment A exploits early to late endosome trafficking machinery, *Mol. Microbiol. 23*, 445−457.
22. Senzel, L., Huynh, P. D., Jakes, K. S., Collier, R. J., and Finkelstein, A. (1998) The diphtheria toxin channel-forming T domain translocates its own NH2-terminal region across planar bilayers, *J. Gen. Physiol. 112*, 317−324.
23. Oh, K. J., Senzel, L., Collier, R. J., and Finkelstein, A. (1999) Translocation of the catalytic domain of diphtheria toxin across planar phospholipid bilayers by its own T domain, *Proc. Natl. Acad. Sci. U.S.A. 96*, 8467−8470.
24. Lemichez, E., and Boquet, P. (2003) To be helped or not helped, that is the question, *J. Cell Biol. 160*, 991−992.
25. Falnes, P. O., and Olsnes, S. (1995) Cell-mediated reduction and incomplete membrane translocation of diphtheria toxin mutants with internal disulfides in the A fragment, *J. Biol. Chem. 270*, 20787−20793.
26. Ratts, R., Zeng, H., Berg, E. A., Blue, C., McComb, M. E., Costello, C. E., vanderSpek, J., Harrison, R., and Murphy, J. R (2003) The cytosolic entry of diphtheria toxin catalytic domain requires a host cell cytosolic translocation factor complex, *J. Cell Biol. 160*, 1139−1150.
27. Ratts, R., Trujillo, C., Bharti, A., vanderSpek, J., Harrison, R., and Murphy, J. R. (2005) A conserved motif in transmembrane helix 1 of diphtheria toxin mediates catalytic domain delivery to the cytosol, *Proc. Natl. Acad. Sci. U.S.A. 102*, 15635−15640.
28. Chenal, A., Savarin, P., Nizard, P., Guillain, F., Gillet, D., and Forge, V. (2002) Membrane protein insertion regulated by bringing electrostatic and hydrophobic interactions into play*A case study with the translocation domain of the diphtheria toxin, *J. Biol. Chem. 277*, 43425−43432.
29. Chenal, A., Nizard, P., Forge, V., Pugniere, M., Roy, M. O., Mani, J. C., Guillain, F., and Gillet, D. (2002) Does fusion of domains from unrelated proteins affect their folding pathways and the structural changes involved in their function? A case study with the diphtheria toxin T domain, *Protein Eng. 15*, 383−391.
30. Zhan, H., Choe, S., Huynh, P. D., Finkelstein, A., Eisenberg, D., and Collier, R. J. (1994) Dynamic transitions of the transmembrane domain of diphtheria toxin: Disulfide trapping and fluorescence proximity studies, *Biochemistry 33*, 11254−11263.
31. D'Silva, P. R., and Lala, A. K. (1998) Unfolding of diphtheria toxin. Identification of hydrophobic sites exposed on lowering of pH by photolabeling, *J. Biol. Chem. 273*, 16216−16222.
32. Malenbaum, S. E., Collier, R. J., and London, E. (1998) Membrane topography of the T domain of diphtheria toxin probed with single tryptophan mutants, *Biochemistry 37*, 17915−17922.
33. Ladokhin, A. S., Legmann, R., Collier, R. J., and White, S. H. (2004) Reversible refolding of the diphtheria toxin T-domain on lipid membranes, *Biochemistry 43*, 7451−7458.
34. Zhao, G., and London, E. (2005) Behavior of diphtheria toxin T domain containing substitutions that block normal membrane insertion at Pro345 and Leu307: Control of deep membrane insertion and coupling between deep insertion of hydrophobic subdomains, *Biochemistry 44*, 4488−4498.
35. Sharpe, J. C., Kachel, K., and London, E. (1999) The Effects of Inhibitors Upon Pore Formation by Diphtheria Toxin and Diphtheria Toxin T Domain, *J. Membr. Biol. 171*, 223−233.
36. Rosconi, M. P., and London, E. (2002) Topography of helices 5−7 in membrane-inserted diphtheria toxin T domain: Identification and insertion boundaries of two hydrophobic sequences that do not form a stable transmembrane hairpin, *J. Biol. Chem. 277*, 16517−16527.
37. D'Silva, P. R., and Lala, A. K. (2000) Organization of diphtheria toxin in membranes. A hydrophobic photolabeling study, *J. Biol. Chem. 275*, 11771−11777.
38. Jain, M. K., and Maliwal, B. P. (1985) The environment of tryptophan in pig pancreatic phospholipase A2 bound to bilayers, *Biochim. Biophys. Acta 814*, 135−140.

39. Berkhout, T. A., Rietveld, A., and de Kruijff, B. (1987) Preferential lipid association and mode of penetration of apocytochrome c in mixed model membranes as monitored by tryptophanyl fluorescence quenching using brominated phospholipids, *Biochim. Biophys. Acta 897*, 1−4.
40. Voglino, L., Simon, S. A., and McIntosh, T. J. (1999) Orientation of LamB signal peptides in bilayers: Influence of lipid probes on peptide binding and interpretation of fluorescence quenching data, *Biochemistry 38*, 7509−7516.
41. Raja, S. M., Rawat, S. S., Chattopadhyay, A., and Lala, A. K. (1999) Localization and environment of tryptophans in soluble and membrane-bound states of a pore-forming toxin from *Staphylococcus aureus*, *Biophys. J. 76*, 1469−1479.
42. Thuduppathy, G. R., Craig, J. W., Kholodenko, V., Schon, A., and Hill, R. B. (2006) Evidence that membrane insertion of the cytosolic domain of Bcl-xL is governed by an electrostatic mechanism, *J. Mol. Biol. 359*, 1045−1058.
43. Brown, W. E., and Wold, F. (1973) Alkyl isocyanates as active-site-specific reagents for serine proteases. Reaction properties, *Biochemistry 12*, 828−834.
44. Cullis, P. R., Fenske, D. B., and Hope, M. J. (1996) in *Biochemistry of Lipids, Lipoproteins and Membranes* (Vance, D. E., and Vance, J. E., Eds.) Elsevier Sciences B.V., Amsterdam.
45. Swairjo, M. A., Seaton, B. A., and Roberts, M. F. (1994) Effect of vesicle composition and curvature on the dissociation of phosphatidic acid in small unilamellar vesicles: A ^{31}P-NMR study, *Biochim. Biophys. Acta 1191*, 354−361.
46. Lepore, L. S., Ellena, J. F., and Cafiso, D. S. (1992) Comparison of the lipid acyl chain dynamics between small and large unilamellar vesicles, *Biophys. J. 61*, 767−775.
47. Korstanje, L. J., van Faassen, E. E., and Levine, Y. K. (1989) Reorientational dynamics in lipid vesicles and liposomes studied with ESR: Effects of hydration, curvature and unsaturation, *Biochim. Biophys. Acta 982*, 196−204.
48. Talbot, W. A., Zheng, L. X., and Lentz, B. R. (1997) Acyl chain unsaturation and vesicle curvature alter outer leaflet packing and promote poly(ethylene glycol)-mediated membrane fusion, *Biochemistry 36*, 5827−5836.
49. van den Brink-van der Laan, E., Killian, J. A., and de Kruijff, B. (2004) Nonbilayer lipids affect peripheral and integral membrane proteins via changes in the lateral pressure profile, *Biochim. Biophys. Acta 1666*, 275−288.
50. Dan, N., and Safran, S. A. (1998) Effect of lipid characteristics on the structure of transmembrane proteins, *Biophys. J. 75*, 1410−1414.
51. Brumm, T., Jorgensen, K., Mouritsen, O. G., and Bayerl, T. M. (1996) The effect of increasing membrane curvature on the phase transition and mixing behavior of a dimyristoyl-sn-glycero-3-phosphatidylcholine/distearoyl-sn-glycero-3-phosphatidylcholine lipid mixture as studied by Fourier transform infrared spectroscopy and differential scanning calorimetry, *Biophys. J. 70*, 1373−1379.
52. Cantor, R. S. (1999) Lipid composition and the lateral pressure profile in bilayers, *Biophys. J. 76*, 2625−2639.
53. Heerklotz, H., and Epand, R. M. (2001) The enthalpy of acyl chain packing and the apparent water-accessible apolar surface area of phospholipids, *Biophys. J. 80*, 271−279.
54. Ladokhin, A. S., and White, S. H. (1999) Folding of amphipathic α-helices on membranes: Energetics of helix formation by melittin, *J. Mol. Biol. 285*, 1363−1369.
55. White, S. H., and Wimley, W. C. (1999) Membrane protein folding and stability: Physical principles, *Annu. Rev. Biophys. Biomol. Struct. 28*, 319−365.
56. Leenhouts, J. M., van den Wijngaard, P. W., de Kroon, A. I., and de Kruijff, B. (1995) Anionic phospholipids can mediate membrane insertion of the anionic part of a bound peptide, *FEBS Lett. 370*, 189−192.
57. Liu, L. P., and Deber, C. M. (1997) Anionic phospholipids modulate peptide insertion into membranes, *Biochemistry 36*, 5476−5482.
58. Parente, R. A., Nadasdi, L., Subbarao, N. K., and Szoka, F. C., Jr. (1990) Association of a pH-sensitive peptide with membrane vesicles: Role of amino acid sequence, *Biochemistry 29*, 8713−8719.

BI602381Z